

# Supporting Information

## Part 1. Tables

**Table S1.** Solubility parameters of CA, acetone and DMAc [1]

Solvents	Solubility parameter (MPa <sup>1/2</sup> )			
	Hansen parameter ( $\delta t$ )	dispersion component ( $\delta d$ )	polar component ( $\delta p$ )	hydrogen bonding component ( $\delta h$ )
CA	25.06	18.60	12.70	11.00
acetone	20.00	15.50	10.40	7.00
DMAc	22.7	16.80	11.50	10.20

**Table S2.** The morphologies of co-electrospun products prepared by different solution couples

Core solution	Shell solution	Core-to-shell flow ratio	Product morphology	Fiber average diameter (nm)
CA-AD21	CA-AD21	1:3	Fibers	302
		1:1	Fibers	238
CA-D	CA-AD21	1:6	Fibers	300
		1:4.5	beaded fibers	221
		1:3	beaded fibers	188
		1:1.5	beaded fibers	107
		1:1	Particles and few fibers	/
		1:0.2	Particles	/
Ag/CA-D	CA-AD21	1:3	beaded fibers	285
		1:1.5	beaded fibers	211
		1:1	beaded fibers	92
PLGA-D	CA-AD21	1:3	Fibers	326
		1:1.5	beaded fibers	238
		1:1	beaded fibers	215
CA-A	CA-D	1:3	Particles	/
		1:1.5	Particles and few fibers	/
		1.5:1	beaded fibers	91
		3:1	beaded fibers	205

## Part 2. Figures

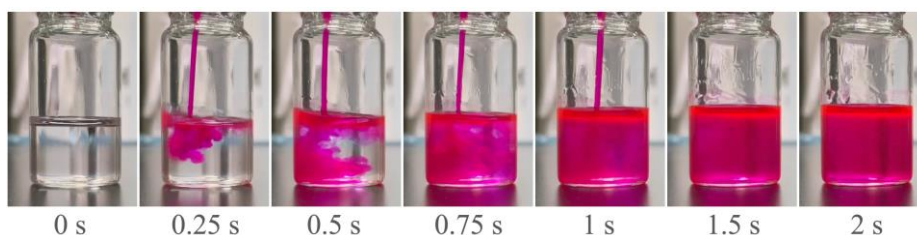


**Figure S1.** The photographs of mixing process between rhodamine/acetone solution and DMAc solvent, showing the high miscibility of acetone and DMAc.

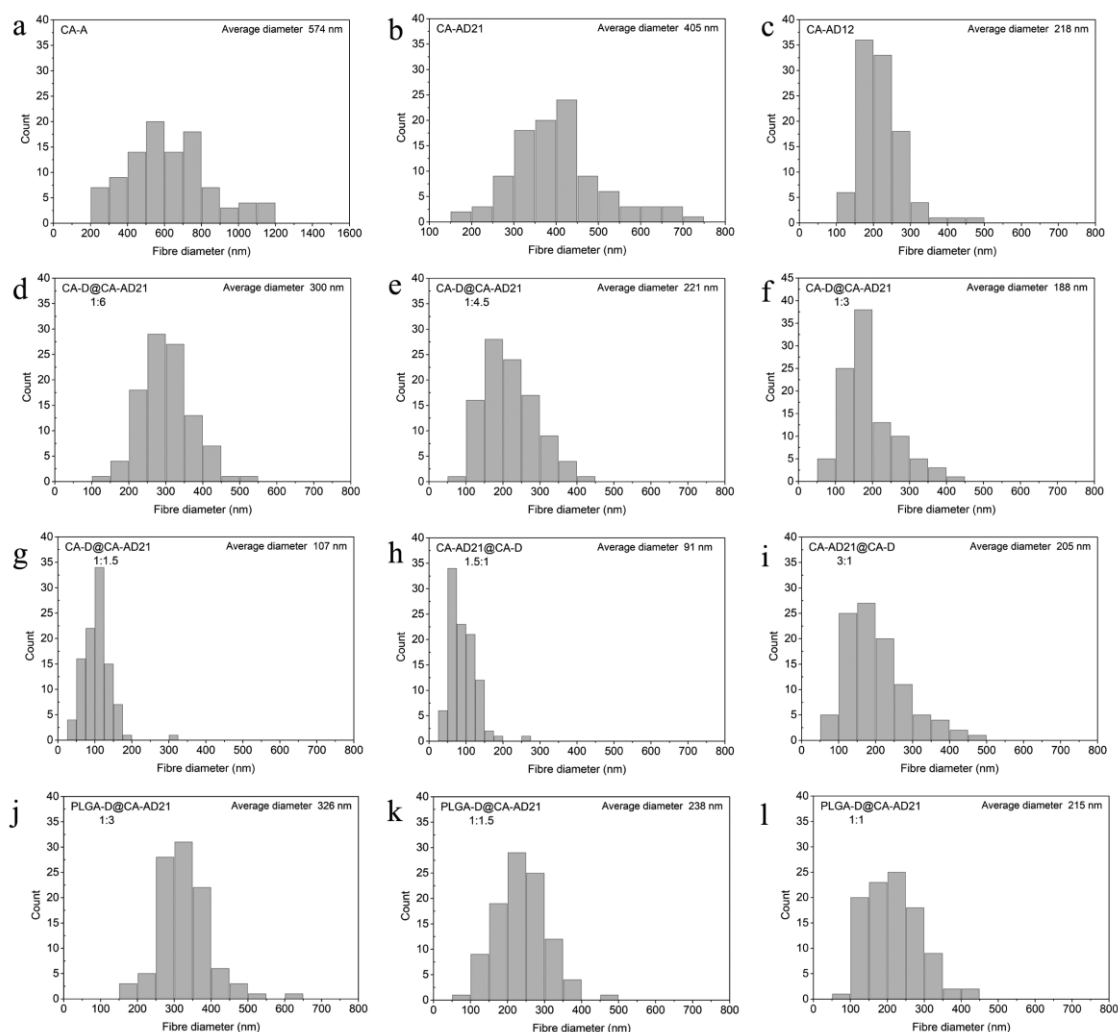


**Figure S2.** The corresponding histograms of fiber diameter. (a)-(c) Single-nozzle electrospinning of (a) CA-A solution, (b) CA-AD12 solution and (c) CA-AD21 solution; (d)-(g) Co-electrospinning of core CA-D and shell CA-AD21 solutions under the core-to-shell flow ratio of (d) 1:6, (e) 1:4.5, (f) 1:3, (g) 1:1.5; (h-i) Co-electrospinning of core CA-A and shell CA-D solutions under the core-to-shell flow ratio of (h) 1.5:1 and (i) 3:1; (j)-(l) Co-electrospinning of core PLGA-D and shell CA-AD21 solutions under the core-to-shell flow ratio of (j) 1:3, (k) 1:1.5 and (l) 1:1.

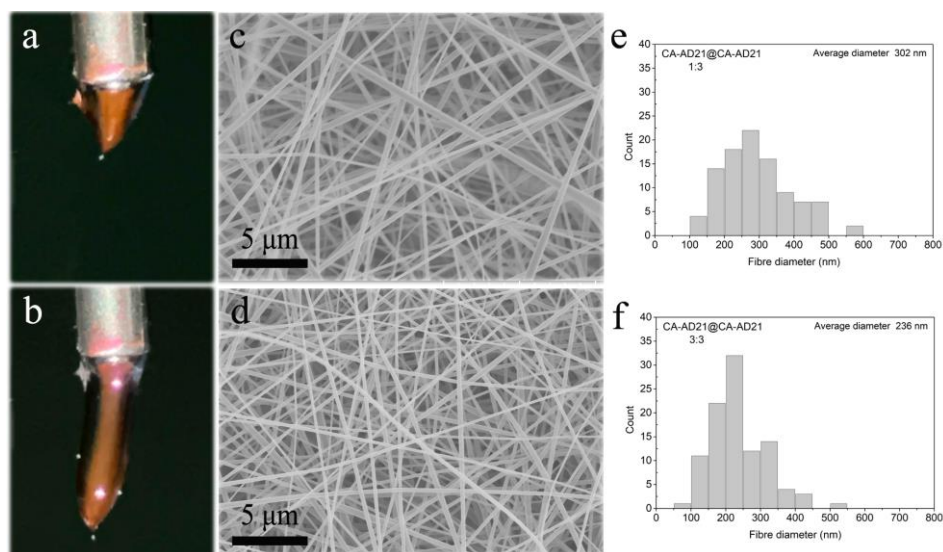


**Figure S3.** (a, b) Images of compound Taylor cones formed in the co-electrospinning of two CA-AD21 solutions under the core-to-shell flow ratio of 1:3 and 1:1. (c, d) SEM images of co-electrospun CA nanofibers corresponding to (a, b). (e, f) The histograms of fiber diameter corresponding to (c, d).

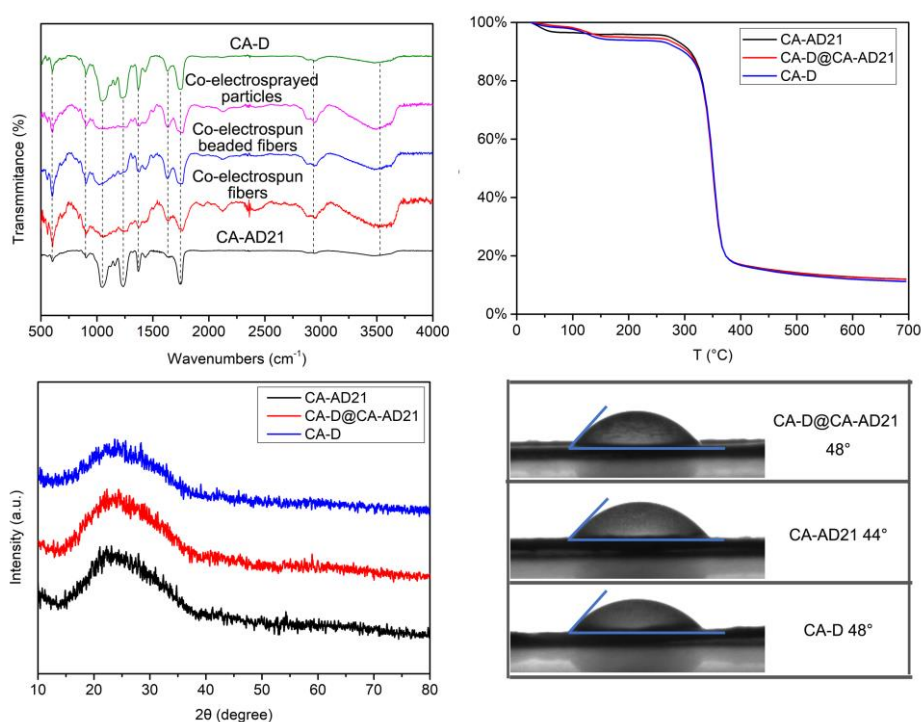


**Figure S4.** (a) FTIR characterizations of the single-nozzle electrospun CA fibers, co-electrospun CA fibers, co-electrospun beaded fibers, co-electrosprayed particles and single-nozzle electrospayed CA particles. (b)-(d) TGA, XRD and contact angle of the single-nozzle electrospun CA fibers, co-electrospun CA fibers and single-nozzle electrospayed CA particles.

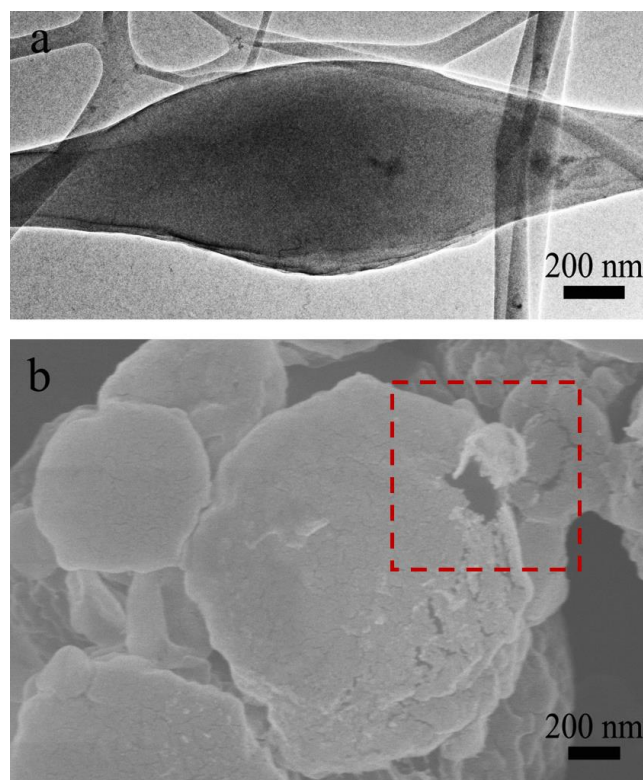


**Figure S5.** (a) A TEM image of a bead and (b) a SEM image of particles prepared by co-electrospinning of CA-D and CA-AD21 solutions.

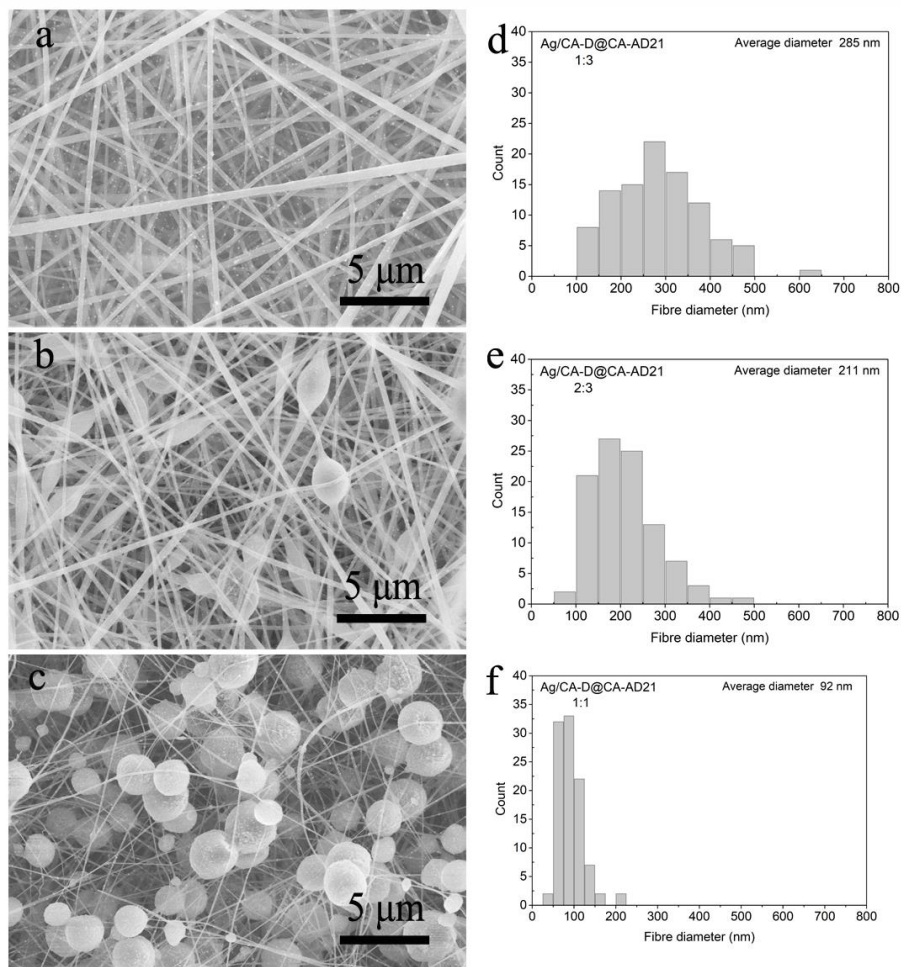


**Figure S6.** (a)-(c) SEM images of Ag-NPs loaded products prepared by co-electrospinning of core Ag-NPs-CA/DMAc solution and shell CA/acetone-DMAc (v/v, 2/1) solution under core-to-shell flow ratio of (a) 1:3, (b) 1:1.5 and (c) 1:1, respectively. (d)-(f) The histograms of fiber diameter corresponding to (a)-(c).

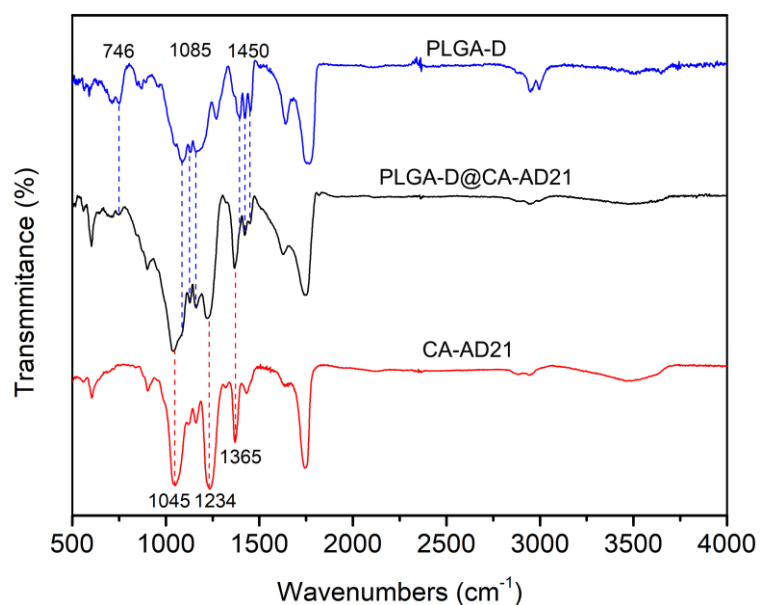


**Figure S7.** (a) FTIR characterizations of the single-nozzle electrospun CA fibers, co-electrospun PLGA@CA fibers and single-nozzle electrosprayed PLGA particles.

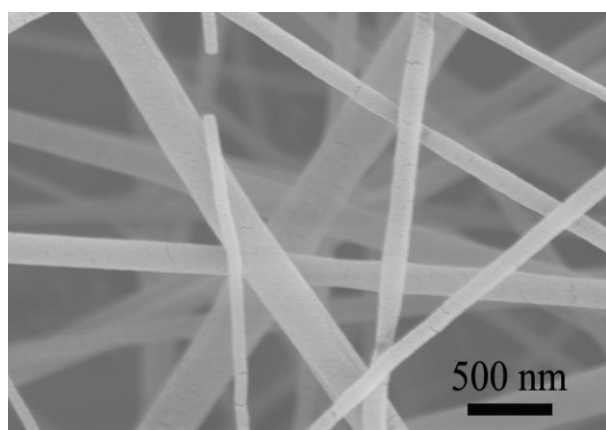


**Figure S8.** A SEM image of nanofibers prepared by co-electrospinning of core CA/acetone solution and shell CA/ DMAc solution under core-to-shell flow ratio of 3:1, showing most nanofibers have a core-shell structure.

## Reference

- [1] Haas D.; Heinrich S.; Greil P. Solvent control of cellulose acetate nanofibre felt structure produced by electrospinning. *J. Mater. Sci.* **2010**, 45, 1299-1306.